

N 62 57599

FILE COPY
NO. I-W

FILE COPY
19

CAST FILE COPY

TECHNICAL MEMORANDUMS

NATIONAL ADVISORY COMMITTEE FOR AERONAUTICS

No. 599

RIVETING IN METAL AIRPLANE CONSTRUCTION

By Wilhelm Pleines

PART IV

From Luftfahrtforschung, Vol. VII, No. 1, April 30, 1930

Washington
December, 1930

FILE COPY

To be returned to
the files of the National
Advisory Committee
for Aeronautics
Washington, D. C.

NATIONAL ADVISORY COMMITTEE FOR AERONAUTICS

TECHNICAL MEMORANDUM NO. 599

RIVETING IN METAL AIRPLANE CONSTRUCTION

By Wilhelm Pleines

PART IV

Strength of Riveted Joints in Duralumin (concluded)

Comparative Tests with Riveted Joints

Subsequent comparison tests were made to determine the crushing strength of a riveted joint, in order to define the difference in crushing strength between a strictly bolted and a riveted joint. These experiments were confined to tests parallel to our Test Series 1 (Part III - N.A.C.A. Technical Memorandum No. 598). Our object was to tabulate the crushing strength by failure on various plate thicknesses for a one-rivet double-shear riveted joint. The dimensions of the specimens were as described in Test Procedure, Part III, page 7. The butt straps were twice as thick as the rivet plate; the shear strength of the rivets was far above the strength of the plates. The rivets were of the same material and were driven within three hours after annealing (See Figure 118, and Table XXXIX).

*"Nietverfahren im Metallflugzeugbau." From Luftfahrtforschung, Vol. VII, No. 1, April 30, 1930, pp. 58-72. For Parts I, II, and III, see N.A.C.A. Technical Memorandums Nos. 596, 597 and 598.

TABLE XXXIX

Dimensions of Test Specimens

Specimen	Plate thickness I	Duralumin 681 B 1/3			
	Plate thickness	b	d	r = e	
	s_1 mm	mm	mm	mm	$\frac{1}{2} d$
a	0.3	18.0	3.1	7.45	2.4 d
b	0.5	18.0	3.1	7.45	2.4 d
c	0.8	24.0	4.1	9.95	2.42 d
d	1.0	30.0	5.1	12.45	2.44 d
e	1.5	36.0	6.1	14.95	2.45 d

TABLE XXXIX (cont.)

Specimen	Plate thickness II	Duralumin 681 B 1/3			
	Plate thickness	b	d	r = e	Bolt hole D
	s_2 mm	mm	mm	mm	mm
a	0.5	18.0	3.1	7.45	6.0
b	0.8	18.0	3.1	7.45	6.0
c	0.8	24.0	4.1	9.95	8.0
d	1.0	30.0	5.1	12.45	10.0
e	1.5	36.0	6.1	14.95	10.0

TABLE XXXX

Crushing Strength by Failure of Riveted Plates
of Varying Thicknesses

Specimen	Mean plate thickness s mm	Hole diameter d mm	Area of hole not riveted $f_t = s d$ mm ²	Ultimate load P_t kg	Crushing strength by failure $\sigma_{LBr} = \frac{P_t}{f_t}$ kg/mm ²
1	0.30	3.1	0.93	118	126.0
2	0.32		0.99	118	119.0
3	0.295		0.92	115	125.0
4	0.29		0.90	119	132.0
14	0.30		0.93	127	136.5
15	0.29		0.90	126	140.0
16	0.29		0.90	123	136.5
17	0.285		0.88	128	145.0
Average	0.30				132.5
6	0.52	3.1	1.62	202	125.0
7	0.515		1.60	189	118.0
9	0.515		1.60	201	125.5
18	0.515		1.60	209	131.0
19	0.53		1.63	196	121.0
20	0.51		1.585	201	127.0
21	0.52		1.62	201	124.0
Average	0.510				124.4
26	0.77	4.1	3.16	356	113.0
27				365	115.5
28				365	115.5
29				362	115.0
Average	0.77				115.0
32	1.05	5.1	5.35	645	120.0
33	1.03		5.25	617	118.0
34	1.05		5.35	675	126.0
35	1.045		5.32	620	116.0
Average	1.045				
38	1.565	6.1	9.55	1073	111.0
39	1.55		9.48	1054	110.5
40	1.55		9.48	1093	115.5
Average	1.558				112.3

Table XXXX shows the mean crushing strength $\sigma_{L Br}$ by failure for the hole wall section before riveting. According to this table there is no premature exhaustion of crushing strength for plates of less than $s = 1$ mm, as in the bolted joints. The specific strength factors were almost the same for all thicknesses. Even the characteristic wavelike formations were absent in the whole riveting series. This verifies the fact that the heads of the rivets and the straps pressed together in riveting, form an excellent support for the plates, and the larger local hole deformations which lower the strength, are avoided. It surely would be commendable to ascertain, by experiments, the effect of the head size of a rivet on the support of the hole walls in rivet plates, and through it, on the crushing strength. The somewhat higher specific crushing strength in the thinner plates is due to the special material quality obtainable in the rolling of thin plates (See Fig. 119).

At various times Professor Gehler, Leipzig, stated when comparing a bolted with a riveted joint, that the twisting of the body within the plastic range of deformation, due to the so-called "clamp" effect, is less in rivets than in bolts. The rivet heads press against the strap plates and form a kind of pin joint for the rivet body, which gives the rivet about 75% more supporting strength than the bolt.

When hammering down the rivet, the hole diameter is usually enlarged, so that the specific strength values, based upon

the nonriveted, original hole cross section, are too high and may lead to fallacious results. For this reason we kept on hand several duplicate specimens of the same groups. The rivet heads were carefully ground off and one strap removed without turning the body in the hole. Then we measured the hole diameter parallel and perpendicular to the direction of the stress with a microscope, up to 1/10 mm accuracy, and estimated to 1/100 mm. The results were 41 enlarged holes, due to clinching (Table XXXXI) - (Compare Table XXIII).

Based upon these hole enlargements the crushing strength by failure $\sigma_{L'Br}$, for

$$\sigma_{L'Br} = \sigma_{BLr} \frac{d_L}{d_L'}$$

is compiled in Table XXXXII, in comparison to the $\sigma_{L Br}$ figures. (The lowered $\sigma_{L'Br}$ values are shown in Figure 119.)

TABLE XXXI

Rivet Hole Enlargements after Clinching

Specimen	Plate thickness s mm	Before clinching		
		Nominal rivet diameter d_E mm	Hole diameter d_L mm	$s d_L$ mm ²
5a	0.3	3.0	3.1	0.93
5	0.3			0.93
12	0.29			0.90
13	0.29			0.90
Average				
10	0.52	3.0	3.1	1.62
11	0.51			1.585
22	0.52			1.62
23	0.51			1.585
Average				
24	0.77	4.0	4.1	3.16
25	0.77			
Average				
30	1.04	5.0	5.1	5.30
31	1.04			
Average				
36	1.54	6.0	6.1	9.39
37	1.55			9.48
Average				

TABLE XXXXI (cont.)

Specimen	After clinching				
	Rivet hole diameter d_L'		Average d_L'	$s d_L'$	$\frac{s d_L'}{s d_L}$
	direction				
	mm	mm	mm	mm ²	
	3.41	3.35	3.38	0.98	1.05
	3.31	3.28	3.30	0.98	1.05
	3.20	3.21	3.21	0.945	1.04
	3.20	3.19	3.20	0.945	1.04
Average			3.26		1.045
	3.24	3.22	3.23	1.72	1.06
	3.32	3.22	3.27	1.68	1.06
	3.39	3.40	3.40	1.72	1.06
	3.39	3.27	3.28	1.68	1.06
Average			3.30		1.06
	4.33	4.30	4.32	3.31	1.05
	4.29	4.26	4.28		
Average			4.30		1.05
	5.38	5.37	5.38	5.51	1.04
	5.20	5.20	5.20		
Average			5.30		1.04
	6.20	6.19	6.20	9.59	1.02
	6.20	6.30	6.25	9.66	1.02
Average			6.23		1.02

TABLE XXXII

Reduced Crushing Strength by Failure Due to Enlarged Hole						
Mean blade thickness s mm		0.3	0.515	0.77	1.045	1.558
Mean crushing strength at failure	σ_{LBr} kg/mm ²	132.5	124.4	115.0	120.0	112.3
	σ_{LBr} kg/mm ²	126.8	117.3	110.0	115.4	110.0

Measurements to Determine the Amount of Hole Enlargement

When the stresses in a simple iron tension plate exceed the limit of safe elastic deformation (yield and elastic limit), the material begins to give in its cross section, i.e., at its critical point. This breaking down is accompanied by continuous reduction in cross section under protracted and increasing stress, and subsequently leads to rupture.

But in riveted joints the conditions are basically different. If the strength of such joints is conditioned by the friction of the plates against each other, caused by rivet head and body (hot riveting), the permanent deformation within the cross section range is likewise small. Permanent deformations of the rivet hole can occur - in cold riveting - when too much clinching enlarges and crushes the hole. And this applies, above all, to cold riveting in light-metal airplane construction (Compare Table XXIII).

Extensive tests have been made regarding the stresses in riveted members and the behavior of riveted joints with respect to elastic and permanent deformations, of which we shall mention the most pertinent data.

In the Schweizer Bauzeitung, Vol. 88, 1926, page 98, Chief Engineer Höhn, Zurich, describes the experiments he had made regarding the elastic behavior of riveted iron plates. As average, he used the stress measurements over plate and strap (See Fig. 120):

The mean stress of the straps is shown in curve a, and of the plates in curve b. At the intersection $a = b$. The dotted line P_L (Figs. 121 and 122) is the so-called line of reference. If there is a difference between the thickness of the plate and that of the straps, the result is a relative displacement between plate and straps, a so-called inner relative shifting. This occurs at each loading, but varies, that is, increases as the distance increases from the line of reference.

The shear in the rivets increases in the same measure, for it is due, and due only to this relative shifting. From elongation measurements in the transverse planes Q_2 , Q_3 , and Q_4 (Figs. 122, 123 and 124), it was found that the rivets of one-half of the respective test specimen were stressed as follows: rivet 1 = 77%; rivet 2 = 7%; rivet 3 = 15%, while the sum of the individual stresses was 100% like a 20-ton load. Curve Q_1 depicts the elongations crosswise to the plate; the middle ordinate must correspond to the 20-ton load.

The inner relative displacements, elastic under normal conditions, are permanent as soon as the member becomes set under higher stress.

But plate and strap can shift for other reasons as well. If a rivet seam becomes loose or even stressed through some other forces, the rivets twist, and we have the so-called "slippage." Höhn calls it outside relative displacement. This occurred at 350-500 kg/mm² shear in the rivets, although 700 kg/mm² represents our present-day limit.

To visualize these procedures we experimented with plate and straps of India rubber and rivets of glass (Fig. 125) for inside relative displacement; plate and straps of glass, rivet of rubber (Fig. 126) for outside relative displacement.

From his experiments, Höhn concluded that the calculation of a rivet seam must be based upon these facts.

Encouraged by these experiments, the author then made a series of tension tests on duralumin rivet joints, in order to determine whether all rivets transmit the tension stresses uniformly and at the same time parallel to the plates under different stages of stress and rivet pitch.

Regarding the size of the safe permanent hole enlargements, very little is known or defined. But the fact that the rivets (in Höhn's tests) under slowly increasing stress remained perfectly fast until failure in one direction, although they were exposed to strong crushing by the higher stress in bending, merits special mention. This unchanged behavior is due to the higher axial force in the body of the rivet with an ensuing strong pressing together of the plates by the rivet heads. We shall refer to this again later.

On the other hand, there is a locally confined over-stress in the riveted joint, followed subsequently by the exceeded range of elastic deformation. For multi-rivet, multiple-row riveting the result is that the differently stressed rivets and rivet holes crush and deform differently, thus causing an inner balance of the stresses and form changes under higher stresses.

Even though we have to accept local permanent deformations, there is still a further purpose in the question of deformation in rivet joints with respect to alternating stresses. Concerning this, Schaechterle emphasizes that the above characterized conditions are essentially different and less favorable in riveted joints exposed to alternating stresses and to direct acting impact forces, so that the danger of loose rivets occurs at stresses below the elastic and the yield limit. An explanation of this question calls for extensive experimentation in repeated stressing of riveted joints. It might be possible to determine the safe stress far enough so that we could speak of the unfitness of a joint when, for instance, the local deformations continuously increase under repeated loading, unloading, or alternate loading.

While describing these tests to determine the safe crushing strength on riveted and bolted joints of duralumin, we pointed out at various times, that local deformations occur through stretching and enlargement of the rivet holes, bulging of plate edges and thickening of hole walls due to crushing

pressure. In particular, the local stretch and enlargement of the hole right up to failure, was quite pronounced, and further tests on the problem of magnitude of enlargement and stretch appear absolutely necessary.

Equally important are the needs for further experiments on the strength of riveted joints and their behavior under impact stresses and stresses with rapid directional changes; the possible effect of greater hole enlargements on the danger of increased impact in alternating stresses, and on impact-like stresses in general. The last may be visualized in cold-riveted joints as having been produced by a preceding loosening of the joints and enlarged rivet holes beyond safety even under steady but inversed stresses with a resulting lack of elastic stress transmission.

The body of the rivet after a certain distance (the free space produced between body and walls) knocks with a certain impact against the hole walls. That these dangers are recognized is shown in the provision which states that duralumin rivets should have only low working strength against impact. Tests of this nature are to be made in the near future, and the results will be published later.

In the following we treat the tests on bolted joints with respect to the amount of permanent hole enlargement and stretching for a) single loading, b) repeated loading and unloading, and c) different loading periods for the individual stages.

In making these tests we used the same bolted joints as shown in Figure 91. The plates were of duralumin (alloy 681B 1/3) plate thickness $s = 1.5$ mm, width b , edge distance e and r , as in our first test series. The holes were drilled 5.9 mm and reamed to 6.0 mm.

We measured the hole enlargements to 1/10 mm exact, and to 1/100 mm estimated, with the microscope. This was made on both sides of the plate in order to forestall the effect of unsymmetrical loading of the hole wall on the magnitude of the uneven hole deformation. As mean enlargement Δd we used the mean of the increase of the original hole diameter.

The results are shown in Figures 127 to 131, with Δd (mm) plotted against the respective load P . Figures 127 to 129 show the Δd values at different stages of loading for single and repeated loading at the same stage and a three-minute period each; Figures 130 and 131 represent the Δd values for different stages P under one short loading (unloaded as soon as stage was reached), followed by a second loading of five minutes each.

Then we photographed the holes in plate No. 4 (Fig. 129) (enlarged 6.6 times). This gave a graphic picture (Figs. 132a-k) of the stretch in the holes under higher stresses. But the most prominent feature is the appearance of the surprisingly high permanent deformation of the holes with respect to the original area, even at low specific crushing strength, in comparison to

our basic $\sigma_L = 60 \text{ kg/mm}^2$ crushing strength. The wings denote original diameter. We are cognizant of the fact, of course, that these tests were made on bolted joints, which does not permit direct comparison to riveted joints. But we are preparing parallel tests for riveted joints so that we shall have comparative figures for both in the near future.

At that, the present results signify that the customary 0.2% limit for safe permanent elongation and yield should be used with reservations. Table XXXXIII shows the Δd values at different load stages in per cent of the original diameter.

Up to $P = 400$ to 450 kg , no effect of load period for the individual stages on Δd was noted, but beyond, Δd showed an increase during the first loading when increasing the period of loading (See Figs. 130 and 131).

TABLE XXXXIII

Enlargement of Holes During Different Load Stages

	Specimen No. Hole diameter d Hole area f_L Ultimate load P_{Br} Crushing strength σ_{LBr}	Crushing pressure for individual stages		Enlargement of Δd	
		P	$\sigma_L = \frac{P}{f_L}$	Total	in % of d
		kg	kg/mm ²	mm	%
Bar 1	$d = 6.03$ mm	150	16.67	0.02	0.33
	$f_L = 9.0$ mm ²	200	22.20	0.035	0.58
	$P_{Br} = 818$ kg	250	28.67	0.040	0.66
	$\sigma_{LBr} = 87.5$ kg/mm ²	300	33.30	0.050	0.83
		400	44.44	0.088	1.46
		500	55.50	0.20	3.30
		550	61.10	0.31	~ 5.10
	600	66.7	0.47	~ 7.8	
Bar 6	$d = 6.02$ mm	150	16.60	0.005	0.083
	$f_L = 9.03$ mm ²	200	22.15	0.025	0.415
	$P_{Br} = 800$ kg	250	27.70	0.040	0.665
	$\sigma_{LBr} = 89.0$ kg/mm ²	300	33.20	0.055	0.91
		400	44.30	0.075	1.25
		500	55.40	0.10 (0.155)	1.66 (2.57)
Bar 7	$d = 6.04$ mm	200	23.10	0.005	0.083
	$f_L = 9.06$ mm ²	250	27.60	0.03	0.50
	$P_{Br} = 790$ kg	300	33.10	0.055	0.91
	$\sigma_{LBr} = 87.5$ kg/mm ²	400	44.10	0.06	~ 1.0
		500	55.20	0.15 (0.16)	2.5 (2.65)

For comparison we again resort to the data of our first test series (See Figs. 96-102) as to elongations in the bolted joints (Fig. 91). Here the permanent elongation of a bolted joint consisting of the same plates yields the figures given in Table XXXXIV.

The measurements of δ comprised the range of the holes and a short plate length.

TABLE XXXIV

Deformation of Plate Edges in Measured Distance δ , (Fig. 91)

Specimen	Hole diameter d Hole area f_L Ultimate load P_{Br} Crushing strength σ_{LBr}	Crushing pressure for individual stages		Permanent elongation δ		
		P	$\sigma_L = \frac{P}{f_L}$	Total	in % of d	
				mm	%	
Bar 11	$d = 6.00$ mm	7.7		0	-	
	$f_L = 9.12$ mm ²	14.3		0.0005	0.0083	
	$P_{Br} = 1030$ kg	20.8		0.0015	0.025	
	$\sigma_{LBr} = 113$ kg/mm ²		27.4		0.003	0.05
			34.0		0.0075	0.125
			40.6		0.027	0.45
			47.1		0.055	0.92
	53.6		0.0970	1.62		
Bar 13	$d = 6.00$ mm	7.7		0	0	
	$f_L = 9.09$ mm ²	14.3		0.0005	0.0083	
	$P_{Br} = 950$ kg	20.8		0.0015	0.025	
	$\sigma_{LBr} = 105$ kg/mm ²		17.5		0.0065	0.110
			34.0		0.0215	0.36
			40.6		0.03	0.65
			47.1		0.063	1.13
	53.6		0.113	1.88		

Assuming uniform loading and even stretching and deformation in both plates the measured δ values apportion themselves to equal parts of the plates in first approximation. The δ values of Table XXXIV already represent hole enlargements at different stages of loading where, of course, the permanent elongation of the small part of the plate included in the measurement is practically negligible. Figure 133 is a graph of the δ and Δd curves plotted against σ_L , by lower σ_L (up to 40 kg/mm²) the values for δ are considerably lower, by $\sigma_L > 40$ kg/mm², as high as the Δd curves.

The deformation of rivet holes due to crushing stresses becomes manifest in the enlarged diameters in the direction of the tension and, at higher Δd and higher stages of loading, in a slight contraction perpendicular to the tension (recognized in wedging of steel bolts on the sides).

In addition to the enlarged holes, the crushing stresses produce crushing and thickening of the hole edge underneath the body of the rivet (acting as bolt). If the rivet heads do not support the walls, the deformation increases and results in bulging in the area of maximum stress (Fig. 134). This continues as the stress increases (See Table XXXVIII) until the hole edges crumble and break, or at least produce the first drop in load prior to breaking (See Fig. 135). Figures 135 to 138 represent various rivet holes shortly before breaking, with their characteristic bulges at the walls which spread to break. The crushing strength by failure for the plates of test series 1 is from 10-20% higher than in the last experiments.

Gehler recently pointed to this area of plastic form changes in the compression zone and recommended a $2.5 d$ instead of a $2.0 d$ edge distance, because the extreme tip of the plastic deformation extends to $1.5 d$ from rivet hole center.

Concluding Remarks

It would be premature to draw any decisive conclusions from these first experiments for permissible hole enlargements and crushing strength factors; to be able to do this requires many more exhaustive tests of similar nature but on riveted joints. Disregarding for the present any possibility of reducing the hole enlargements as a consequence of plate support through the heads of the rivets, we are justified in saying, after these tests, that $\sigma_L = 60$ to 70 kg/mm² is a safe crushing strength by failure. As to maintaining the 0.2% limit we remain silent, because at 12/1000 mm this limit is already reached by $\sigma_L = 18$ to 35 kg/mm². Assuming 1% = 60/1000 mm as permanent local load, values of $\sigma_L = 33$ to 46 kg/mm² could still be considered safe. Should we confine our decision as to fitness or unfitness of riveted joints solely to that point at which holes continue to become larger under repeated loading and unloading, our limit would already be reached at $\sigma_L = 50$ to 55 kg/mm², without consideration of the absolute measure of the hole enlargements for this stress.

Another point of view leads us to look into the problem of safe crushing pressure a little more in detail and to point a way to more uniform strength specifications. According to the tests on safe crushing pressure (Part II, following Table XXII - N.A.C.A. Technical Memorandum No. 597) the crushing strength by failure $\sigma_L Br$ (with $\sigma_L \text{ safe} = 2.5 \sigma_{\text{safe}}$, for safe crushing

pressure σ_{safe} , according to Table XXXV) yielded the following values:

TABLE XXXV

Crushing Strength for Steel 48 and Steel 37

Specimen	Steel 48	Steel 37
Plate thickness t mm	12.0	12.0
Hole diameter d mm	23.0	23.0
Hole area $t d$ mm	276.0	276.0
Mean crushing pressure by failure P_{Br} kg (for $e = 2.5 d$ and $r = 2.0 d$)	36,350	28,200
Crushing strength by failure $\sigma_{L Br} = \frac{P_{Br}}{t d}$ kg/mm ²	131.7	102.2
Safe stress σ_{safe} kg/mm ² (State railway specifications)	18.2	14.0
Safe crushing strength $\sigma_{L safe} = 2.5 \sigma_{safe}$ kg/mm ²	45.5	35.0
Ratio $\frac{\sigma_{L Br}}{\sigma_{L safe}}$	2.90	2.92

According to this, the limit of permissible crushing pressure for steel plates Steel 48 and Steel 37, used as rivet plates is:

$$\sigma_{L safe} = \left(\frac{1}{2.9} \text{ to } \frac{1}{3} \right) \sigma_{L Br}$$

If we apply the same limit values to the present material our tests on riveted joints of duralumin (See beginning of this report) would result in

$$\sigma_{L \text{ Br}} = \sim 110.0 \text{ kg/mm}^2 \text{ (See test data, Table XXXXII)}$$

$$\sigma_{L \text{ safe}} = \sim \frac{1}{3} \sigma_{L \text{ Br}} = \sim 37.0 \text{ kg/mm}^2$$

Since the theoretical crushing strength in German metal airplane construction corresponds to approximately half of the tensile strength (See Part II - W.A.C.A. Technical Memorandum No. 597), the safety against rupture is amply sufficient.

But the ideas as to the admissibility of these railway specifications are far from agreement in technical circles, as shown by the objections registered in B. Kunze's report.*

It is pointed out that the specified safe crushing pressure $\sigma_{L \text{ safe}} = 2.5 \times \sigma_{\text{safe}}$ was too high, because - assuming the same safety - the ratio (factor of safety)

$$\frac{\sigma_{L'}}{\sigma_{L \text{ safe}}} \text{ would have to be the same as } \frac{\sigma}{\sigma_{\text{safe}}} \text{ in tension members,}$$

if $\sigma_{\text{safe}} =$ safe tension stress (kg/mm²),

$\sigma =$ yield point (kg/mm²),

$\sigma_{L \text{ safe}} =$ safe crushing pressure (kg/mm²),

$\sigma_{L} =$ crushing strength (kg/mm²), for which the deformation curve shows a distinct bend (See Fig. 90).

The rivet plates (steel 48) used by the state railway, showed:

$$\sigma = 33.8 \text{ kg/mm}^2,$$

$$\sigma_{\text{safe}} = 18.2 \text{ kg/mm}^2.$$

and a

$$\frac{\sigma}{\sigma_{\text{safe}}} = \frac{33.8}{18.2} = 1.86 \text{ factor of safety.}$$

B. Kunze, "Zulässiger Lochleibungsdruck." Die Bautechnik, No. 7, Feb. 17, 1928.

The mean crushing strength was $\sigma_L = 65.0 \text{ kg/mm}^2$. Likewise, since

$$\frac{\sigma_L}{\sigma_{L \text{ safe}}} = 1.86,$$

$$\sigma_{L \text{ safe}} = \frac{65}{1.86} = 34.9 \text{ kg/mm}^2$$

and

$$\sigma_{L \text{ safe}} = \frac{34.9}{18.2} \sigma_{\text{safe}} = 1.92 \sigma_{\text{safe}}$$

for the ratio

$$\alpha = \frac{\sigma_{L \text{ safe}}}{\sigma_{\text{safe}}}$$

For the same reasons, Krohn advocated as safe crushing pressure the double shear stress

$$\sigma_{L \text{ safe}} = 1.6 \sigma_{\text{safe}}$$

From the reports read at the Second International Bridges and Superstructures meeting at Vienna, September 24-27, 1928, we quote from the treatise of S. Gallik and Findeisen on shearing strength and crushing pressure in bolted and in riveted joints:

With d = diameter of rivet,

e = edge distance from plate center in direction of tension,

σ_l = crushing pressure,

σ = tearing strength of plate material,

we have $\frac{\sigma_l}{\sigma} = \frac{e}{d}$. This formula has been checked by numerous

experiments, and the failures invariably occurred in the direction of the plate axis.

In order to prevent plate fracture by slitting lengthwise to the plate and to make the break occur at right angles to the plate axis (transverse fracture) the above formula was to be changed to

$$\frac{e}{d} = 1.10 \frac{\sigma_l}{\sigma}$$

which, theoretically, means that σ_l may be of arbitrary size, providing e is large enough. But this really formulates an upper limit for the crushing strength, because the plate is heavily upset under crushing pressure. If this continues, the plate tears or the rivet heads snap off, for which reason Gehler advocated $\sigma_l = 2 \sigma$ as upper limit, while Dornen established $\sigma_l = 3 \sigma$ as safe crushing pressure in his experiments.

At the meeting it was proposed to select $\sigma_l = 2.3 \sigma$ as safe crushing pressure by $e = 2.5 d$ edge distance.

Findeisen also grants that the riveted joint might be superior to a bolted joint, but he objects to the high $\alpha = 2.5$, while at $\alpha = 2.0$ the crushing pressure in bolted joints already begins to look serious. He is of the opinion that the question of necessary safety needed more attention and some decisive action when formulating a suitable value for α .

Gehler stressed the necessity of increased caution in strictly bolted joints with respect to the crushing strength, and deems $\sigma_l = 1.5 \sigma_{\text{safe}}$ appropriate.

In contrast to this Weidmann asserts that a higher crushing strength factor is permissible because:

1. The stress due to crushing pressure is locally confined to a small portion of the plate, while the remaining plate is stressed in its whole cross section.

2. The deformations at entry and when exceeding the crushing strength are in the first instance small and locally confined, and spread but little within the material.

A p p e n d i x

Experiments to Determine the Stress Distribution in a Multiple-Row Riveted Joint

Motive.— In the calculation of a riveted joint, it is very important to know how the individual rivets in a multiple and multi-riveted joint transmit the stresses, and to what extent the individual rivets contribute to the support by suitable selection of rivet spacing and row spacing.

But it has never become common practice to assume the total loading of a riveted joint as evenly distributed over the individual rivets and to proceed upon this assumption.

Some preliminary experiments in this connection were begun by the D.V.L. in 1927, but had to be discontinued. Before referring to these in detail, mention may be made of a very detailed description of a riveted joint under stress and its ensuing effect. Using Bleich's assumptions, we examine a five-

rivet, double-row, lap-rivet joint (Fig. 139).

Some considerations on the theory of riveted joints, with special reference to the calculation of the force distribution over the individual rivets in a single-row rivet joint (axially stressed plates) (according to Bleich).

In Figure 139 we note that:

S' (kg) = stress in plate at (I) between two adjacent rivets, say, S_3' between rivets 3 and 2;

S'' (kg) = stress in plate in section (II) between the same rivets;

f' and f'' = the cross sections in same section of (I) and (II).

We assume that:

1. Both rivets have equal cross sections, i.e., $f_1' = f_2' = \text{constant} = s b$;
2. All rivets are evenly spaced;
3. All rivets are of equal size and thickness, t ;
4. The slippage is negligible.

(This, in particular, applies to metal airplane construction, where cold riveting is used.) The stress is simply transmitted by the shear and bending resistance of the rivets.

Applying a stress to this riveted joint we have, due to stress P , longitudinal stresses σ_I in plate (I), which - according to the amount in which P is transmitted to plate (II) by rivets 1 to 5 - decrease in the order of the rivets from 1 to 5, as the distance from the point of the applied force increases. Consequently, σ_I is maximum in front of the

first rivet in section (I) and zero behind rivet 5.

The same stress conditions apply to plate (II), only the decrease of σ_{II} in plate (II) is reversed. Figure 140 is a graphic presentation of the qualitative stress distribution.

A general rule for each plate section between two adjacent rivets is, that the sum of the stresses in two adjoining plates must equal the stress corresponding to the total stress. Now our general equation of equilibrium reads as

$$S_n' + S_n'' = P \tag{1}$$

when n is computed from 1 to 6, and in our case (See Fig. 139)

$$S_1' + S_1'' = S_2' + S_2'' = S_3' + S_3'' = \dots = S_6' + S_6'' = P$$

A second equation is derived from the following:

Each rivet transmits a certain force N , which we shall call rivet force. But N must equal the change in plate force S from a section ahead of to the section behind the respective rivet, conformal to the different stresses in these parts, so

$$N_n = S_n' - S_{n+1}' \tag{2}$$

where n is computed from 1 to 6.

Thus, we have, for example, for rivet 3

$$N_3 = S_3' - S_4' = S_4'' - S_3''$$

Now Bleich proves that:

1. The end rivets have greater force, and the force decreases toward the center;

2. The greatest rivet forces occur on the side where the stronger of the two plates ends;
3. The high percentage of force contribution to be taken up by end rivets in the case of more than six rivets, remains almost constant, so that any greater number than six is of no advantage;
4. Plate sections decreasing toward the ends involve smaller differences in rivet forces.

Object of Experiment

When we determine the stress distribution in the individual plate sections between two adjacent rivets, we can define the forces S in the individual stress panels, as well as the individual rivet forces. Of course it is difficult to give a decisive, quantitative determination of stress and rivet force distribution for riveted joints of light metal, on account of the prevailing small dimensions.

Preparation and Test

The dimensions of the duralumin rivet joint, the pitch, size of rivets, etc., can be seen in Figure 139. The elongations were measured in the central axis in the different rivet panels (Fig. 139) (spacing $e = 30$ mm) of both plates. We used a Fuess tensiometer, and $l = 20$ mm as edge distance. The measurements were repeated several times, i.e., for reloading

and unloading, and the average determined. A test took seven minutes.

The stresses are as follows:

Hooke's law is valid within the range of elastic deformation, so

$$\frac{\Delta l}{l} = \alpha \sigma$$

where l = measured length,

Δl = extension of l ,

$$\alpha = \frac{1}{E} = \frac{1}{700000},$$

σ = the tension.

Consequently,

$$\sigma = \frac{E}{l} \Delta l = K \Delta l$$

K in this case is

$$K = \frac{E}{l x}$$

where x - the transmission (estimated to $1/10$ mm) = 1 : 60000.

Accordingly

$$K = \frac{700000}{2.0 \times 60000} = 5.83$$

and

$$\sigma = 5.83 \Delta l \quad (\text{kg/mm}^2).$$

R e s u l t s

The computed stress σ in the symmetrical axis of both plates is shown graphically in Figures 141 to 143.

Figures 141 and 142 show the mean stress σ plotted against stress P for plates (I) and (II) in the sections between two adjacent rivets. Figure 143 depicts stress σ in the different panels (central axis) between the adjacent rivets at various load stages within the range of elastic form changes.

C o n c l u s i o n s

(See Figures 141-143)

The conclusions applicable to any stress within the range of elastic deformation are:

1. The stress in the symmetrical planes of the individual panels between two adjacent rivets shows an almost linear increase with the loading.
2. The greater the distance of the individual panels between two adjacent rivets from the point of application of the loading, the lower the stress. The stress is maximum in the panel ahead of the first rivet, although the stress decrease does not occur quite evenly with the increase in panel spacing, but this irregularity in the two plates is in all probability due to the difference in material strength and insufficient accuracy in measurement.

Assuming, for rough calculation, a constant stress distri-

bution in the individual panels between two adjacent rivets, the decrease in stress in the individual panels is similar to that shown in Figure 144 for $P = 500$ kg and plate (I).

So when we compute S in the different panels, we have

$$S = \sigma q_1,$$

where

$$q_1 = \text{constant} = 1.5 \times 30.0 = 45 \text{ mm}^2,$$

and the stress in each panel becomes:

$$S_{f1} = 10.5 \times 45.0 = 475 \text{ kg}$$

$$S_{e1} = 7.3 \times 45.0 = 330 \text{ "}$$

$$S_{d1} = 5.5 \times 45.0 = 250 \text{ "}$$

$$S_{c1} = 3.8 \times 45.0 = 170 \text{ "}$$

$$S_{b1} = 2.0 \times 45.0 = 90 \text{ "}$$

$$S_{a1} = 1.6 \times 45.0 = 70 \text{ "}$$

The equilibrium equation requires that rivet force N be equal to the change of the force in the plates in two adjacent panels. So the cursory calculation yields for rivets 1, 2, and 3, the following rivet force:

$$N_1 = S_{f1} - S_{e1} = 475 - 330 = 145 \text{ kg}$$

$$N_2 = S_{e1} - S_{d1} = 330 - 250 = 80 \text{ "}$$

$$N_3 = S_{d1} - S_{c1} = 250 - 170 = 80 \text{ "}$$

We included the decrease in rivet force by increasing distance from the point of application of force P within range of elastic deformation, in Figure 144. It will be seen that

the outer rivets have to absorb the greatest force, while the stress decreases toward the rivet seam.

Although these preliminary experiments are not to be taken as giving conclusive evidence of the behavior of a riveted joint, they nevertheless should prove of invaluable aid to the designer in his selection of correct riveted joints, rivet spacing, etc.

Translation by J. Vanier,
National Advisory Committee
for Aeronautics.

References

- Bach, C. v. : "Elastizität und Festigkeit."
- Bach, C. v. : "Maschinenelemente," Vol. I.
- Bach, C. v. and Baumann, R. : "Festigkeitseigenschaften und Gefügebilder der Konstruktionsmaterialien."
- Bach, C. v. and Baumann, R. : "Versuche zur Klarstellung des Einflusses der Spannungen, welche durch das Nieten im Material hervorgerufen werden, und die der Entstehung von Nietlochrissen Vorschub leisten können," Zeitschrift des Vereines deutscher Ingenieure, 1912, p. 1890.
- Baumann, R. : "Versuche zur Ermittlung der in den Blechen beim Nieten bewirkten Formänderungen." Zeitschrift des Vereines deutscher Ingenieure, Forschungsheft No. 252.
- Baumann, R. : "Das Wesen der Nietverbindung." Der Bauingenieur, 1925, No. 2.

- Beck, R. : "Duralumin, seine Eigenschaften und Verwendungsgebiete." Z. f. Met., Vol. 16, (1924), p. 122, 1927.
- Bleich, : "Theorie und Berechnung der eisernen Brücken," p. 260.
- Bohner and Westlinning, : "Das Nieten von vergütbaren Aluminium-Legierungen." Z. f. Met. 20. (1928), p. 209.
- Brenner, I., : "Lautal als Baustoff für Flugzeuge. Bericht der D.V.L., Berlin-Adlershof, Luftfahrtforschung, Vol. I, No. 2, Feb., 1928.
- Dörnen, : "Die bisherigen Anschlüsse steifer Fachwerkstäbe und ihre Verbesserung, " 1924. Wilhelm Ernst and Son, publishers.
- Höhn, E. : "Nieten und Schweissen der Dampfkessel." Julius Springer, Pub.
- Kaiser, H. : "Untersuchungen über die Wirkung von Anfangsspannungen in Nieten und Schrauben." Zeitschrift des Vereines deutscher Ingenieure, 1914, p. 1402 and following pages.
- Kunze, B. : "Zulässiger Lochleibungsdruck." Die Bau-technik, Vol. VI, No. 7, Feb. 17, 1928, pp. 91, 92.
- Meissner, K. L. : "Das Altern veredlungsfähiger Aluminiumlegierungen bei erhöhten Temperaturen." Z. f. Met., Vol. 17, 1925, p. 81.
- Meissner, K. L. : "Die Veredelungsvorgänge in vergutbaren Aluminiumlegierungen." Zeitschrift für Flugtechnik und Motorluftschiffahrt, 1926, No. 17, p. 112.
- Preuss, : "Die Spannungsverteilung an gelochten Zugstäben." Zeitschrift des Vereines deutscher Ingenieure, 1912, p. 1780, etc.

- Preuss, : "Versuche an Nietungen." Zeitschrift des Vereines deutscher Ingenieure. 1912, p. 404, etc.
- Rettew, H. F. and Thumin, G. : "Tests on Riveted Joints in Sheet Duralumin." N.A.C.A. Technical Report No. 165, 1923.
- Rudeloff, M. : "Versuche mit Nietverbindungen und Brückenteilen." Verhandlungen des Vereins zur Beförderung des Gewerbfleisses 1911, Report III.
- Schaechterle, K. : "Die Nietverbindungen bei Brücken aus hochwertigen Stählen." Die Bautechnik, Vol VI, No. 7, Feb. 17, 1928, pp. 81-84; and No. 8, Feb. 24, 1928, pp. 96-98.
- Weidmann, : "Versuche über den zulässigen Lochleibungsdruck von Nietverbindungen." Die Bautechnik, Vol. V, No. 46, Oct. 21, 1927.
- Weidmann, : "Erwiderung." Die Bautechnik, Vol. VI, No. 7, Feb. 17, 1928.
- Weidmann, : "Beanspruchung der Bleche beim Nieten." Zeitschrift des Vereines deutscher Ingenieure, 1922, p. 501.
- Findeisen, : "Scherfestigkeit und Lochleibungsdruck von Bolzen- und Nietverbindungen." Bauingenieur, 1929, No. 12.
- Gehler, : "Bericht über die II. Internationale Tagung für Brücken- und Hochbau in Wien." Bautechnik, 1928, No. 51.
- Pietzker, : "Festigkeit der Schiffe," Berlin 1911, p.88. Mittler and Son, Pub.

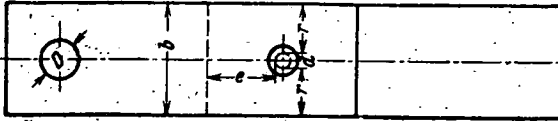
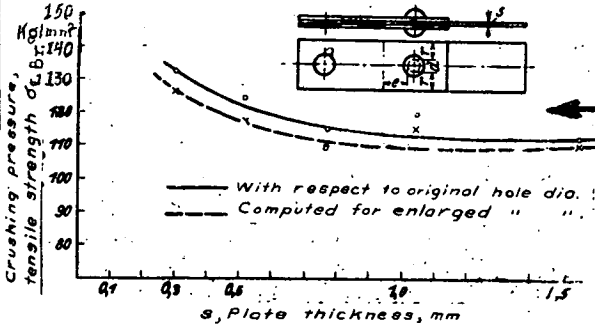
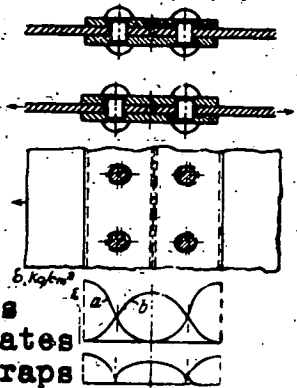


Fig. 118 Dimensions of single rivet specimen.



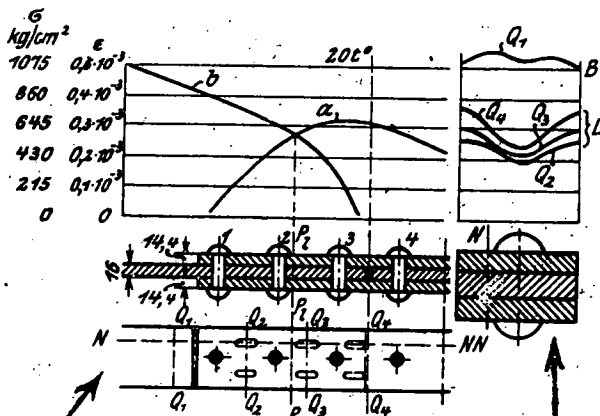
123 124 125 126
133 134 139

Fig. 125 Inner relative shifting.



Relative shifting between plate and straps
a, Stretch of plates
b, Stretch of straps

Fig. 119 Crushing pressure-tensile strength of riveted plates. Highest in thin plates in contrast to bolted joints. Head of rivet supports hole walls against bulging.



Figs. 120-122 Longitudinal distribution in plate (b) and strap (a)

Figs. 123-124 Transverse stress distribution in plate (B) and straps (L).

Figs. 120-124 Mean shape of stress in plate and strap. (Bohn measurements)

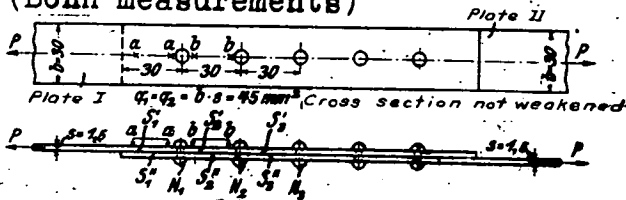


Fig. 139 Plate and rivet forces in single shear, multiple row riveted joint.

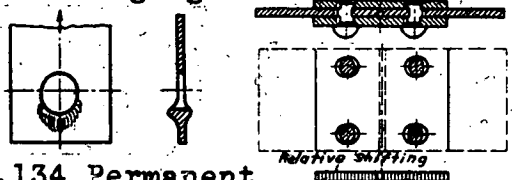


Fig. 134 Permanent crushing Fig. 126 Outer of stressed edges relative shifting.

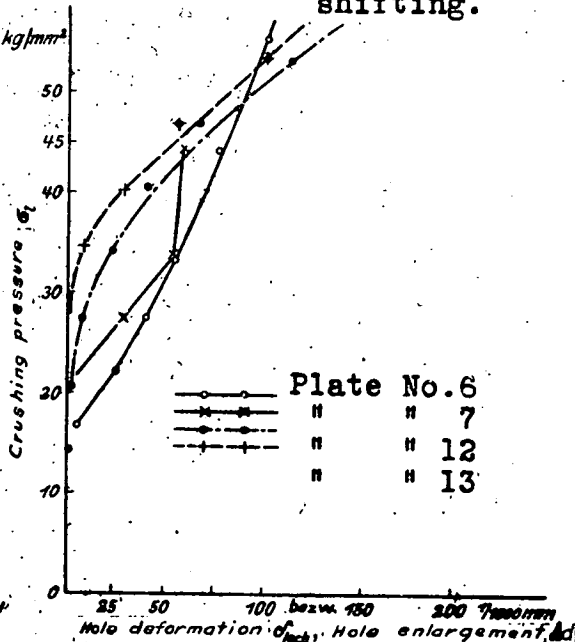


Fig. 133 Comparison of hole deformation and enlargement. (Assuming $\delta_{loch} = \frac{\delta_{measured distance}}{2}$)

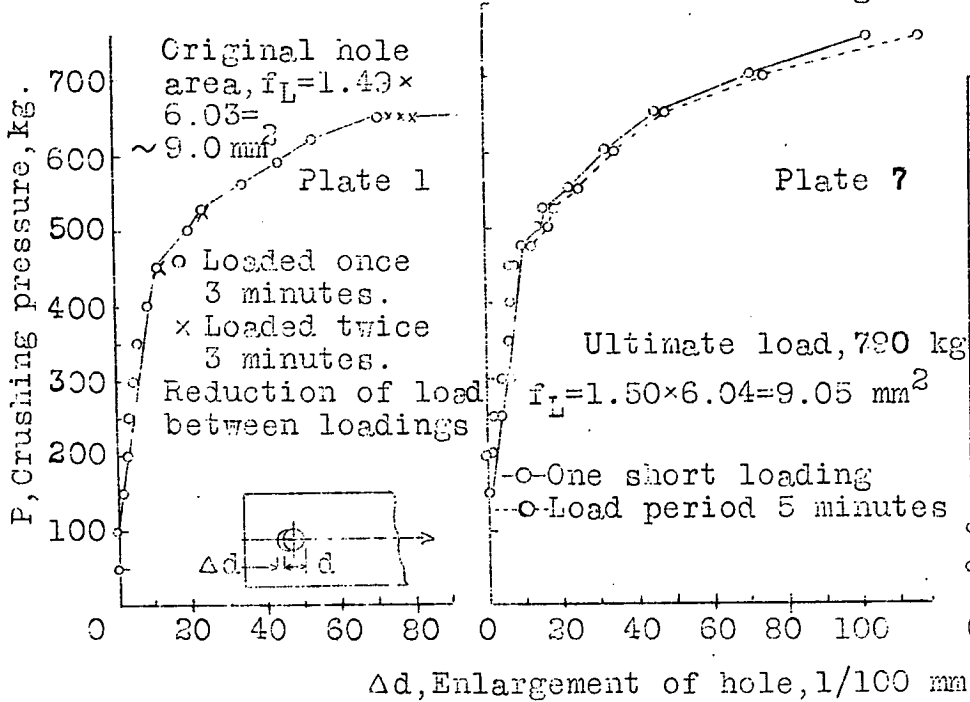


Fig. 127

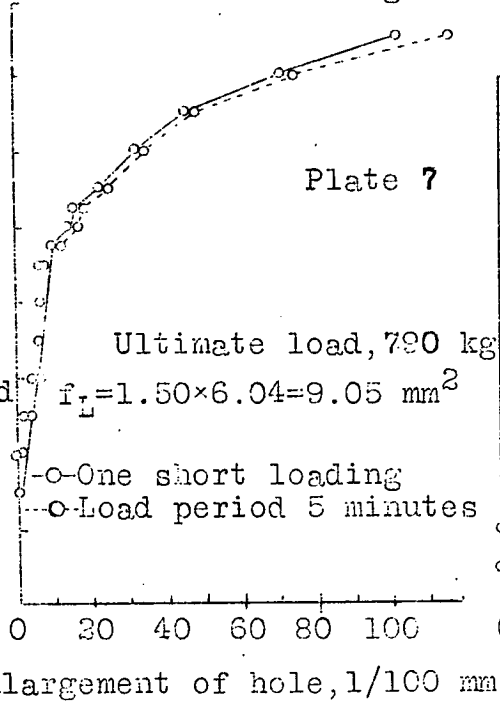


Fig. 131

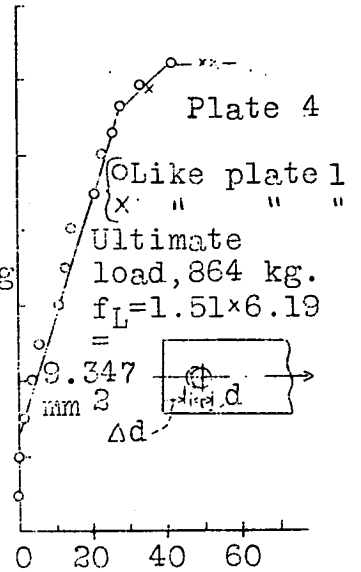


Fig. 129

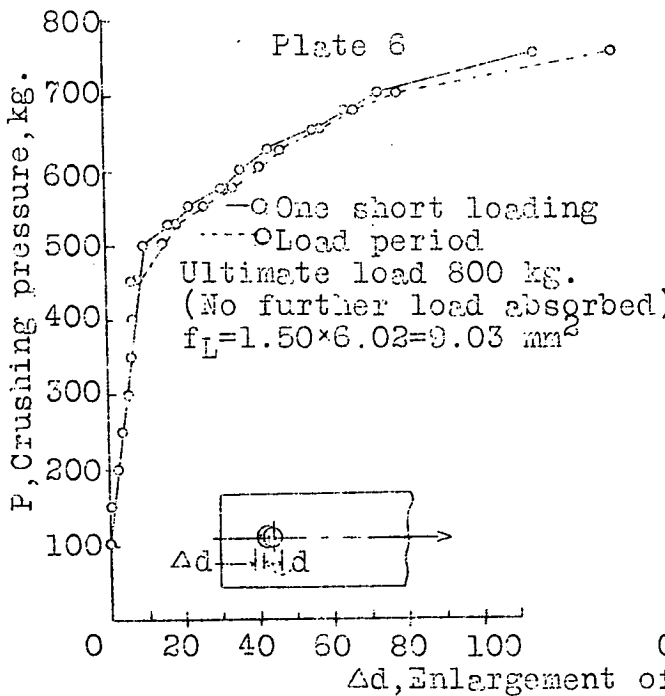


Fig. 130

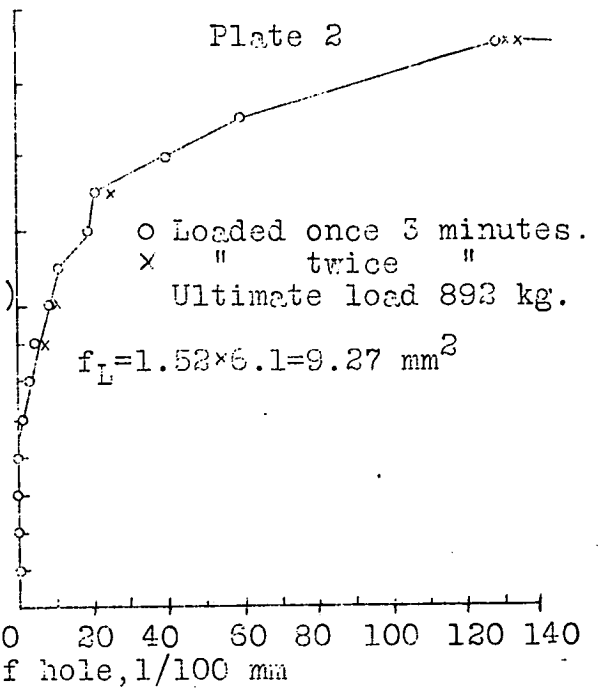
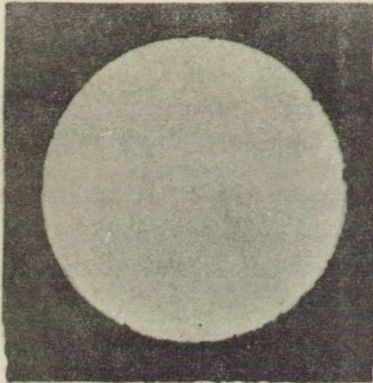


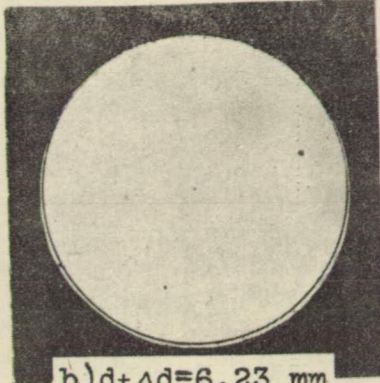
Fig. 128

Figs. 127-131 Enlargement of holes plotted against crushing pressure at various load stages and periods.

Result, Very high hole enlargements at low crushing pressures.



a) $d=6.19$ mm, $P=0$ kg.



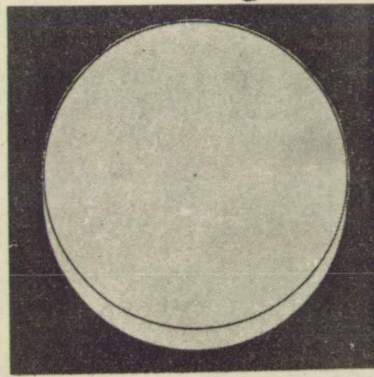
b) $d+\Delta d=6.23$ mm
 $P=200$ kg.



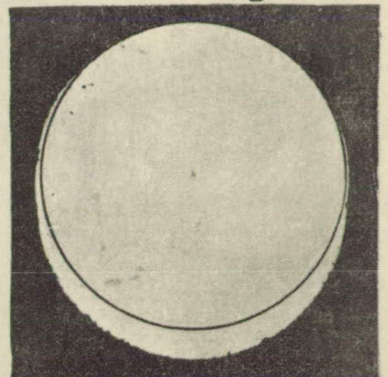
c) $d+\Delta d=6.30$ mm
 $P=300$ kg



d) $d+\Delta d=6.42$ mm
 $P=500$ kg.

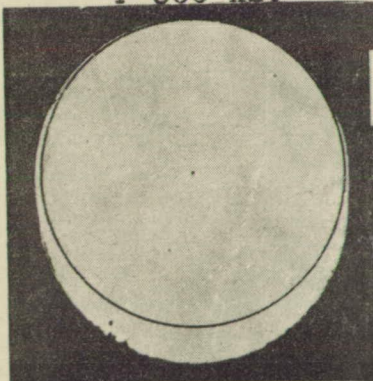


e) $d+\Delta d=6.54$ mm, $P=590$ kg.

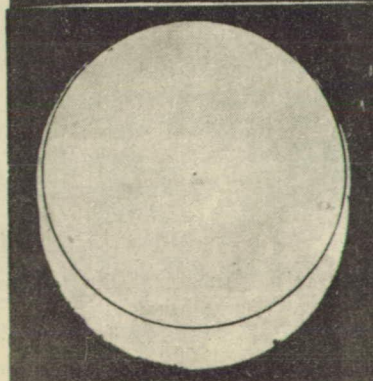


f) $d+\Delta d=6.71$ mm

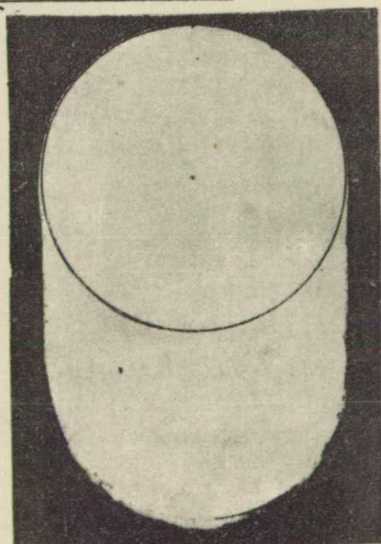
e, f) (after 2×3 minute load period) $P=620$ kg.



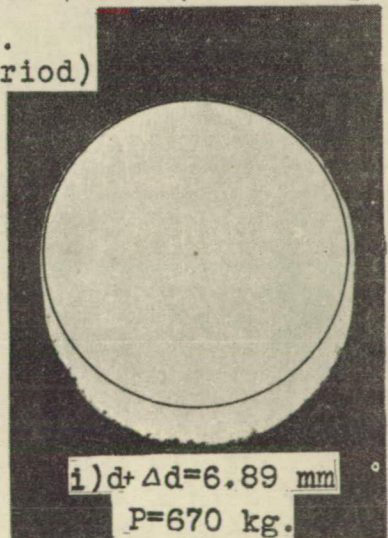
g) $d+\Delta d=6.81$ mm $P=670$ kg.
(after 2×3 min. load period)



h) $d+\Delta d=6.86$ mm $P=670$ kg. (see Fig. 145)
(after 5×3 min. load period)



k) $d+\Delta d=rd.10$ mm $P=rd.850$ kg.
(ready to break)



i) $d+\Delta d=6.89$ mm
 $P=670$ kg.
(after 6×3 min.
load period)

Fig. 132a k
Photographs
of enlarged holes at
various stages of
loading. (Magnified
about 6 times).

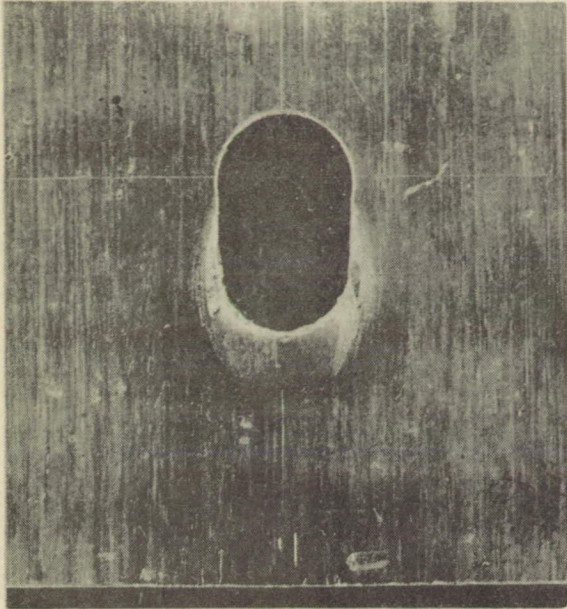


Fig.135 Hole deformations due to crushing pressure before break.

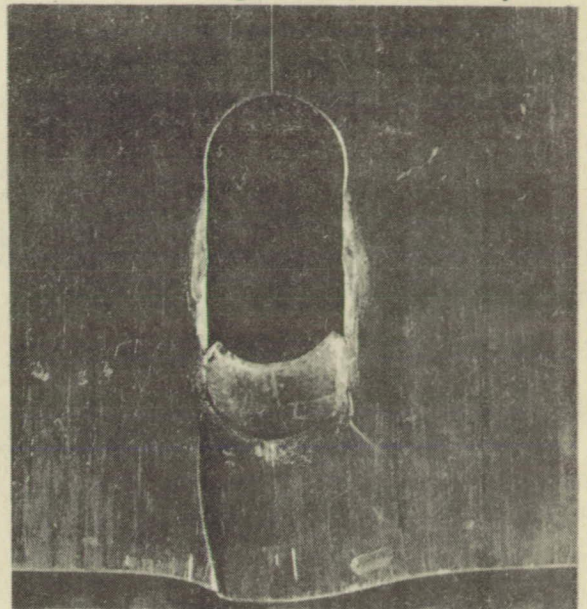


Fig.136 Hole deformations due to crushing pressure before break.

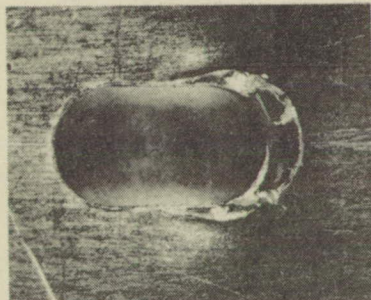


Fig.138 Break due to stress in crushing pressure.

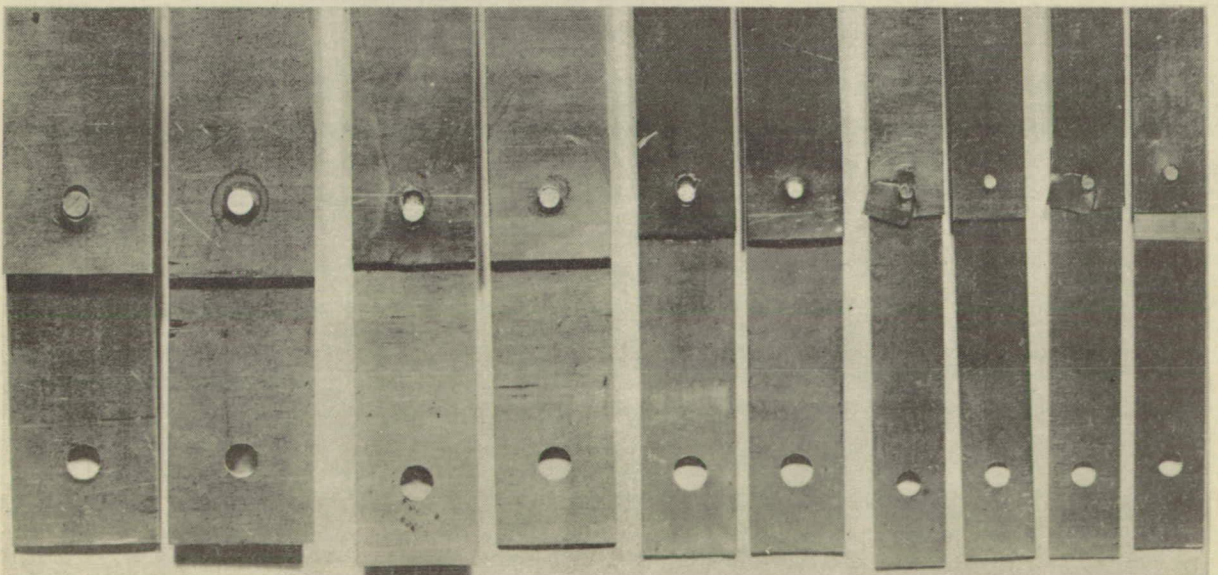


Fig.137 Hole enlargements after clinching and at failure due to stress in crushing pressure.

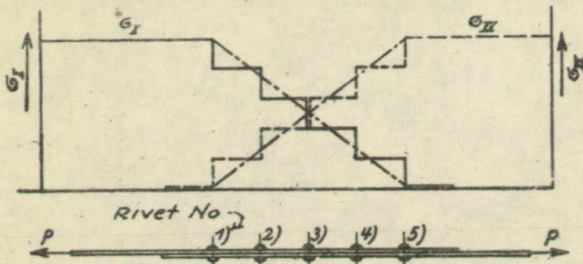


Fig.140 Usual stress distribution in single shear, multiple row riveted joint.

— For uniformly distributed load σ in each panel between adjacent rivets.
 - - - For rectilinear drop of σ

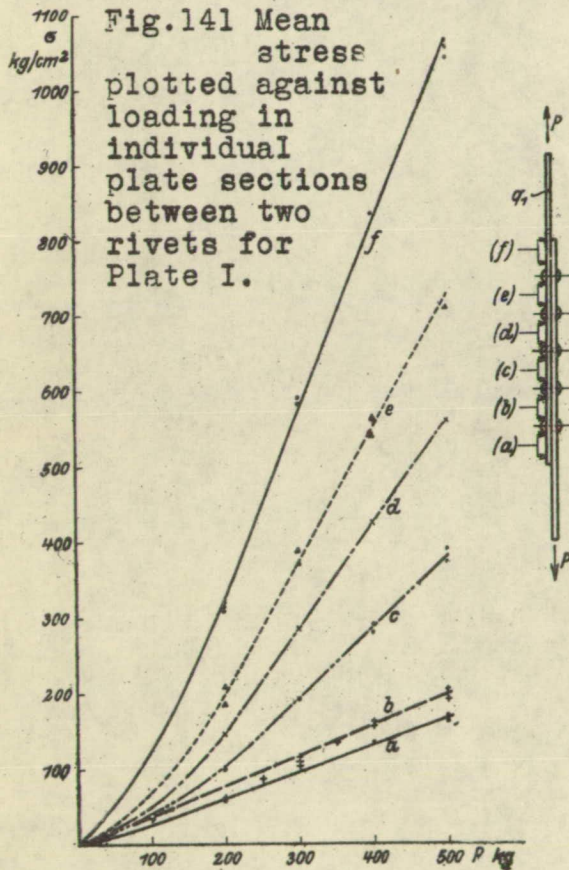


Fig.141 Mean stress plotted against loading in individual plate sections between two rivets for Plate I.

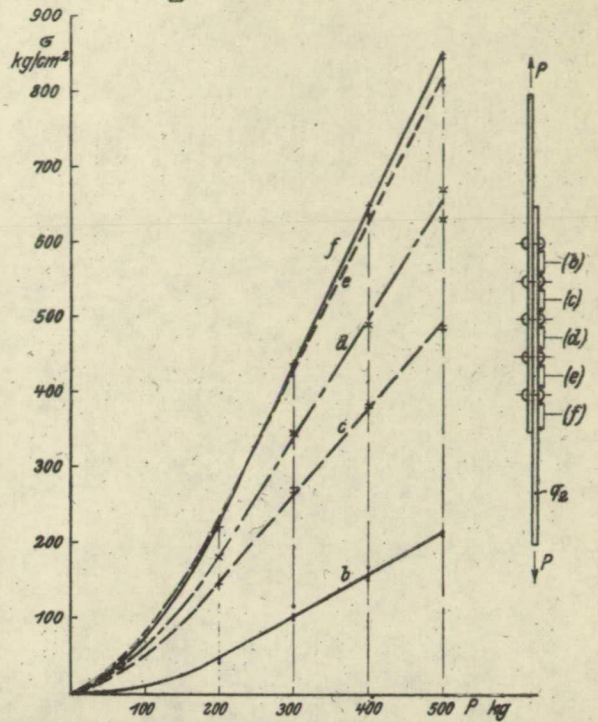


Fig.142 Mean stress plotted against loading in individual plate sections between two rivets for plate II.

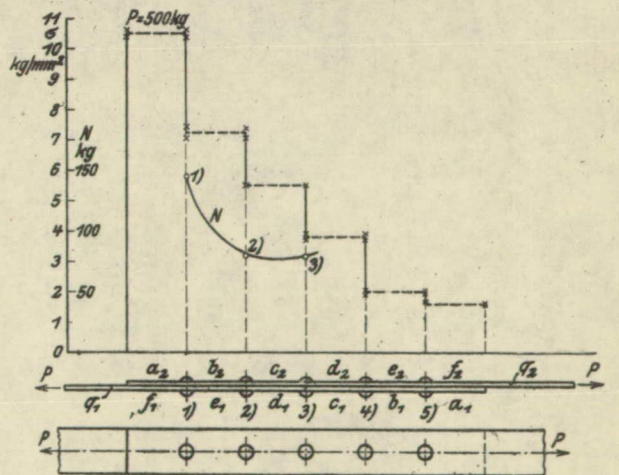


Fig.144 Stress distribution in plates and in individual panels and magnitude of rivet forces for a definite stage of loading.

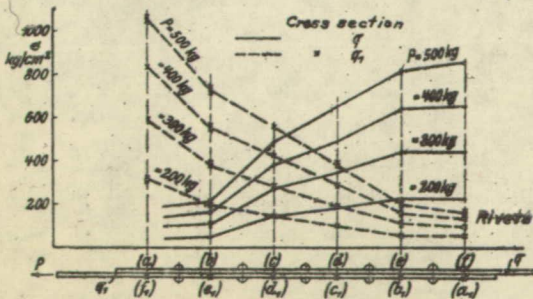


Fig.143 Mean stress in individual plate sections (central axis) between two rivets in a single shear riveted joint.